

## **A COMPACT UWB ANTENNA WITH DUAL BAND REJECTION**

**P. Tilanthe<sup>1,\*</sup>, P. C. Sharma<sup>2</sup>, and T. K. Bandopadhyay<sup>3</sup>**

<sup>1</sup>Department of EC, TRUBA College of Engineering and Technology, Indore, India

<sup>2</sup>Department of ECE, S. D. Bansal College of Technology, Indore, India

<sup>3</sup>Department of ECE, Bansal Institute of Science and Technology, Bhopal, India

**Abstract**—In this communication, a new compact UWB monopole antenna with dual band rejection is presented. The antenna is designed using FR4 substrate with dielectric constant 4.4, loss tangent 0.02 and a height of 1.59 mm. Initially the UWB antenna is designed to obtain a 153% fractional bandwidth from 2.4 GHz–21.7 GHz. The ground plane beneath the patch is etched out and a rectangular slot is introduced to obtain a broadband matching over the operating frequency range. Later the antenna is modified to get a frequency notch in the IEEE802.11a and HIPERLAN/2 WLAN operating band (5.15 GHz–5.825 GHz) to avoid potential interference. A U shaped slot is optimally introduced in the patch to get the desired performance. Finally an L shaped slot is cut from the radiating patch to filter the frequency band 3.3 GHz–3.6 GHz, which is WiMAX service band. The antenna parameters are optimized and the effects of parametric variation on antennas performance are studied and the summary is presented. The antenna is fabricated and measured results are presented. The measured results are in well agreement with the simulated results.

---

*Received 22 September 2011, Accepted 27 October 2011, Scheduled 2 November 2011*

\* Corresponding author: Pramendra Tilanthe (pramendra20@yahoo.com).

## 1. INTRODUCTION

UWB is a fast emerging technology for short range communication enabling extremely high data rate for transmitting very low energy level broadband pulses. Since the Federal Communication Commission FCC has distributed the unlicensed band of 3.1 GHz–10.6 GHz for UWB communications [1], the UWB systems are evolving as a potential candidate for wireless technology. Consequently UWB antennas are getting considerable attention from both researchers and industries worldwide [2–4] due to the advantages associated with it, such as high data rates, invulnerability to multipath fading and extremely low spectral power density [5, 6]. However unlike the design of traditional microstrip antenna, design and analysis of UWB antennas is more challenging and difficult. A good UWB antenna should be capable of operating over the bandwidth assigned by the FCC. At the same time a small and compact antenna size is highly desirable, due to the integration requirement of UWB systems. Also reasonable efficiency and satisfactory radiation properties over the entire frequency range are necessary. Another key requirement of UWB antennas is good time domain behavior, i.e., a good impulse response and minimal distortion [7]. An UWB system requires the inclusion of band rejection filters to avoid possible interference from existing wireless local area networks (WLAN), allocated from 5.15 GHz to 5.825 GHz. However, the required WLAN band rejection can be incorporated directly at the antenna to avoid the addition of band rejection filters in the UWB system.

Presently some research work has been reported for UWB antennas designed for military and commercial applications. In a recent publication [8], Yazdanifard et al. have demonstrated a new stepped square monopole antenna with W shaped slot and a ground plane with rectangular sleeves and a pair of L-shaped resonator for an ultra wide bandwidth of 130% (3.05 GHz–14.3 GHz). In yet another recent publication [9], a square monopole antenna is presented with a pair of T-shaped slot and a ground plane with a pair of rectangular sleeves and T-shaped resonator to provide an ultra wide fractional bandwidth of more than 125% (3.05–13.57 GHz). Jiang et al. [10] have presented a novel compact broadband antenna which can radiate from 2.8 GHz to 18.6 GHz with frequency notched characteristics at 5.2 GHz. A few good examples of UWB antennas may also be found in [11–15]. However, most of the recently reported papers give the simulated and experimental results of frequency domain characteristics of the UWB/band notched UWB antenna like return loss, VSWR, gain, radiation pattern in  $E$  plane and  $H$  plane [8–15]. In order to

completely characterize a UWB antenna, time domain characteristics are also important like impulse response, signal fidelity etc. CST MICROWAVE STUDIO™ [21] is used for the design and optimization of antenna, which is based on method of finite integration technique (FIT). In this paper a new stepped square monopole antenna is proposed and to achieve WLAN bands rejection, a U shaped slot is introduced in the patch. To achieve WiMAX band rejection another slot is introduced in the patch. Time domain characteristics of the antennas are discussed as well. The organization of the paper is as follows. Section 2 describes the geometry of the earlier designed UWB antenna and its measured results. Section 3 discusses the simulated and optimized of the WLAN band notched UWB antenna. Section 4 summarizes the final design with dual notch rejection. Lastly the findings of the investigation are discussed.

## 2. UWB ANTENNA DESIGN

The geometry of the antenna (referred to antenna-A in this communication) is presented in Figure 1.

The total size of the antenna including the ground plane is  $40 \times 36 \text{ mm}^2$ , which is printed on a FR4 glass epoxy substrate of thickness 1.59 mm, and relative permeability of 4.4. The photograph of the fabricated UWB antenna is shown in Figure 2.

The patch having dimension  $W \times L$  is excited using an offset 50 ohms microstrip line. The dimension of the offset feed is  $W_f \times l_f$  whereas the feed is offset by 1.75 mm from the patch center. Slots are cut from the edges of the patch in stepped manner with the dimensions  $W_{s1} \times L_{s1}$ ,  $W_{s2} \times L_{s2}$ ,  $W_{s3} \times L_{s3}$  and  $W_{s4} \times L_{s4}$ . The impedance

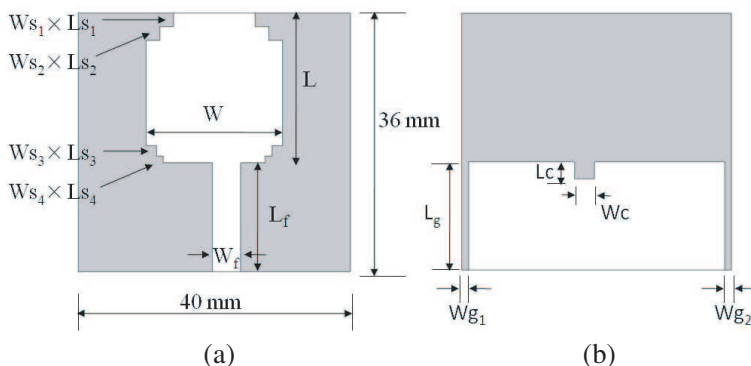


**Figure 1.** Configuration of proposed UWB antenna (antenna-A). (a) Top view. (b) Bottom view.

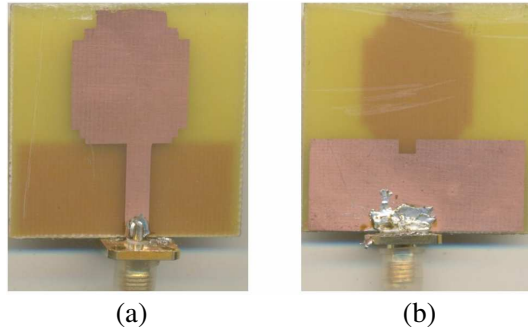


**Figure 2.** Fabricated prototype. (a) Top view. (b) Bottom view.

**Table 1.** Details of proposed antenna's parameters.

Antenna Component	Symbols and their values for the proposed antenna (in mm)
Patch	$W = 20, L = 22$
Feed	$W_f = 4.2, L_f = 16$
Upper Steps	$W_{s1} = 2, L_{s1} = 2, W_{s2} = 2, L_{s2} = 2$
Lower Steps	$W_{s3} = 1.5, L_{s3} = 1.5, W_{s4} = 1, L_{s4} = 1$
Ground	$L_g = 16$
Ground Slot	$W_c = 3, L_c = 2.5, W_{g1} = 1, W_{g2} = 1$
Substrate	Width = 40, Length = 36

bandwidth is the most important characteristics of an ultra wide band antenna. The length of ground plane being  $L_g$ , and a rectangular cut is introduced in the partial ground plane, exactly beneath the feed line with a dimension of  $W_C \times L_C$ , in order to provide wide band matching of the transmission system with the radiator. The antenna parameters are optimized in order to obtain a good impedance match and stable radiation characteristics with high gain over an ultra wide frequency band. The two rectangular slots with dimension  $W_{g1}$  and  $W_{g2}$  which are cut from ground plane results in bandwidth enhancement and ground area reduction. The final values of the optimum parameters are indexed in Table 1.

### 2.1. Results of UWB Antenna

The ultra wideband antenna is designed and fabricated and the return loss characteristics are measured. The proposed antenna exhibits good

UWB characteristics with wide operating range of 2.4 GHz to 21.7 GHz with a fractional impedance bandwidth of more than 153%. The experimentally measurement of its return loss was done by Rohde & Schwarz vector network analyzer. The plots of simulated and measured reflection coefficient are shown in Figure 3 for the antenna parameters indexed in Table 1. The frequency of operation of the patch antenna as a function of the patch width along with its length can be given as “[16]” —

$$f_{r,nm} = \frac{c}{2\sqrt{\epsilon_{r,eff}}} \left[ \left\{ \frac{n}{L + 2\Delta L} \right\}^2 + \left\{ \frac{m}{W + 2\Delta W} \right\}^2 \right]^{1/2} \quad (1)$$

In this equation,  $L$  and  $W$  are the patch length and width respectively,  $\Delta L$  and  $\Delta W$  are incremental length and width which account for the fringing of the field at respective edges. Whereas  $c$  is the speed of light,  $\epsilon_{r,eff}$  is the permittivity of the dielectric substrate and  $n, m = \{0, 1, 2, \dots\}$  are the number of half cycle field variation along the patch length and width, respectively.

As observed from Figure 3, the first resonance frequency (3 GHz) of the radiator, at which the value of  $S_{11}$  is  $-30$  dB is determined by rectangular patch dimensions  $L$  and  $W$  and is governed by Equation (1). The antenna operates in  $TM_{10}$  mode at this frequency and it behaves as a quarter wave monopole antenna. The second, third and fourth pole frequencies are 6.2 GHz, 7.9 GHz and 9.9 GHz, at which the value of  $S_{11}$  are  $-34$  dB,  $-36$  dB and  $-39$  dB respectively. Due to these pole frequencies the antenna exhibits an UWB response. As observed from Figure 3, the value of  $S_{11}$  is well below  $-10$  dB throughout the UWB frequency band. From simulation results, the lower cutoff frequency is found to be 2.8 GHz while it is 2.4 GHz as

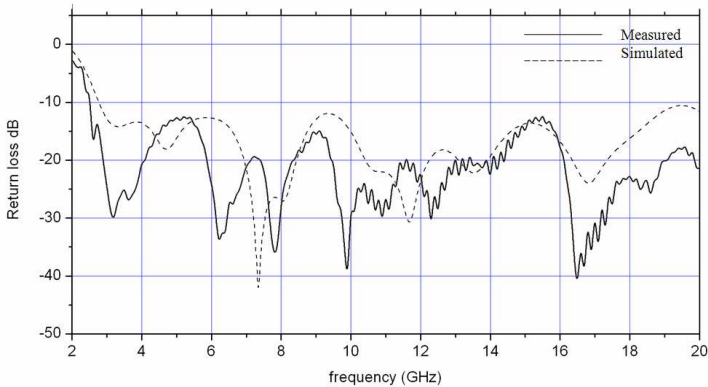


**Figure 3.** Comparison of simulated and measured return loss.

obtained from the measured results. It is observed that the dimension of the slot present in the ground plane beneath the microstrip line is the most crucial parameter for getting the broad bandwidth as well as proper impedance matching to maximize the antennas radiation efficiency. The optimized value of length of this slot is 2.5 mm and that of the width is 3 mm. As observed from simulation results, the proposed antenna exhibit radiation behavior up to 21.7 GHz but the testing and measurement facility available was up to 20 GHz. Therefore the measured results are presented only up to 20 GHz.

As observed from Figure 4, the real part of antenna impedance is exactly 50 Ohms at many frequencies within the overall UWB band which are 2.6 GHz, 3.3 GHz, 4.6 GHz, 6.25 GHz, 7.1 GHz, 7.75 GHz, 8 GHz, 9.4 GHz, 10.2 GHz, 12.4 GHz, 13.9 GHz, 15.7 GHz, 18.4 GHz, 21 GHz and 22.4 GHz. It shows the multi resonance behavior of the antenna. Also the real part of the antenna impedance varies from 25 Ohms to 71 Ohms whereas the imaginary part of the antenna impedance is in the range of  $-24$  Ohms to  $+25$  Ohms which is not a major variation of the antenna impedance.

The  $E$  plane and  $H$  plane radiation patterns of the proposed monopole UWB antenna at various pole frequencies i.e., 3 GHz, 6.2 GHz, 10 GHz and 16.2 GHz are computed and the same are shown in Figures 5(a)–(b) respectively. It can be observed that the  $E$ -

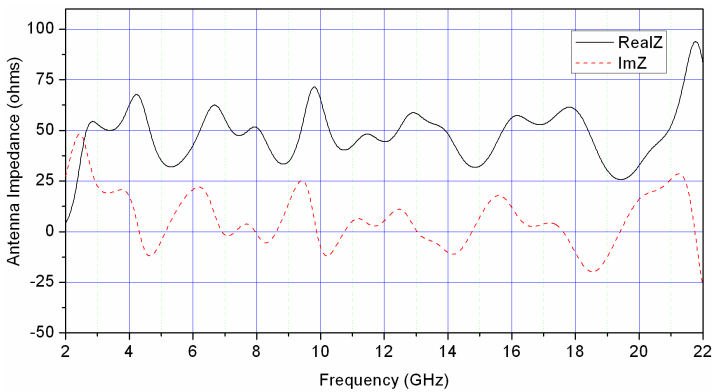


**Figure 4.** Antenna impedance versus frequency curve for proposed UWB antenna.

**Table 2.** Parameters of U-shaped slot (all dimension in mm).

$X_1$	$X_2$	$X_3$	$X_4$	$Y_1$	$Y_2$
1.2	9.6	1.2	4	5.7	4

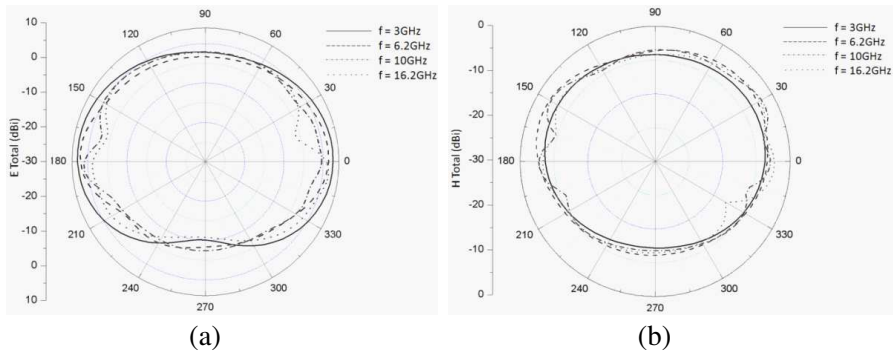


**Figure 5.** (a) *E* plane pattern and (b) *H* plane pattern for UWB antenna.

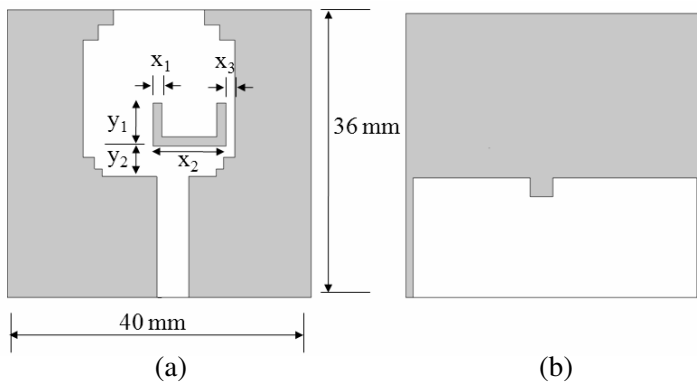


**Figure 6.** Geometry of proposed UWB antenna with WLAN notch (antenna-B). (a) Top view. (b) Bottom view.

plane radiation pattern is almost stable throughout the UWB. It has maximum directivity at 12 GHz that is 6.22 dBi and minimum directivity at 4.7 GHz which is 3.3 dBi. The *H* plane pattern is not purely omnidirectional but is almost stable throughout the UWB. It is observed that both *E* and *H* plane patterns deteriorates a little bit as the frequency increases.

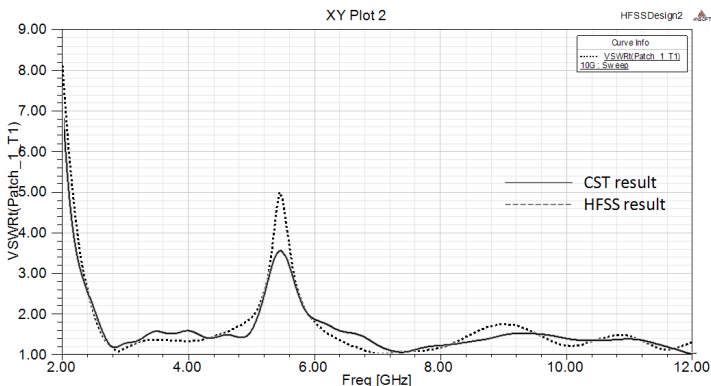
### 3. UWB ANTENNA WITH A SINGLE FREQUENCY BAND NOTCH

The geometry of the antenna-A is modified by introducing a U shaped slot in the radiating element and the same is given in Figure 6. Except

from the U-shaped slot, all the other dimension of the substrate, feed, ground plane, ground slot etc., are kept the same. The total length of the U-slot is  $\lambda/2$  at the center frequency of the WLAN frequency band. As a design point of view, it is easy to tune the notch center frequency by selecting the total length of U-slot. The parameters of the U slot are given as  $X_1$ ,  $X_2$ ,  $X_3$ ,  $Y_1$  and  $Y_2$ . The optimized values of these parameters are given in Table 2. The offset of the U-slot center from that of the patch at the right hand side is named as  $X_4$ . This parameter plays a key role in deciding the optimum WLAN band rejection. The antenna will be termed as antenna B throughout the discussion.

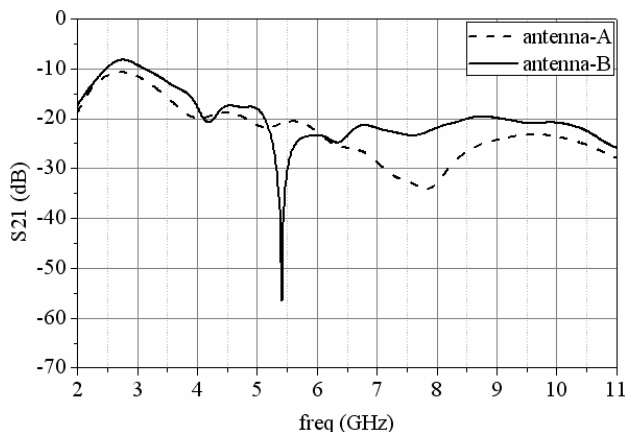
### 3.1. Frequency Domain Results

Figure 7 shows the VSWR characteristics of the antenna. The CST results are validated using EM software HFSS [22]. A good agreement is observed between the results obtained from two different EM solver techniques. It is observed that in the WLAN band (5.15 GHz–5.825 GHz), a notch is obtained in the return loss characteristics of the earlier designed UWB antenna (antenna-A) if an optimized U-slot is introduced (with the parameter values given in Table 2). It is noted that for WLAN frequency band, the values of VSWR are greater than 3. In the surface current analysis simulation, it has been observed that, at frequencies 3.5 GHz and 7 GHz the current distribution is mainly along the transmission line and very small around the U-slot. While at 5.5 GHz, the majority of current is distributed around the U-slot only, which means that, a destructive interference occurs between the forward and reverse traveling waves and the antenna becomes



**Figure 7.** VSWR of antenna-B.





**Figure 8.** Comparison of Insertion loss ( $S_{21}$ ) for proposed antennas.

nonresponsive at this frequency.

In order to compute the transfer function of the proposed UWB antennas, the similar antennas are positioned in a transmit-receive system at a distance of 50 mm. This type of system can be considered as a two port network where knowledge of the parameter  $S_{21}$  contains the information of all the system parameters such as gain, impedance matching, polarization matching and phase delay. As observed from Figure 8, the  $S_{21}$  for antenna-A has a value  $-14$  dB at 3.1 GHz and  $-25$  dB at 10.6 GHz. The  $S_{21}$  characteristic is below  $-30$  dB from frequency 7.6 GHz to 8.1 GHz with a dip at frequency 7.8 GHz, at which  $S_{21}$  is  $-32$  dB. Except this frequency band, the  $S_{21}$  characteristics almost lies in between  $-20$  dB to  $-30$  dB in the entire UWB band which is just satisfactory and cannot be called as an excellent  $S_{21}$  UWB performance. On the other hand, antenna-B exhibits much satisfactory performance in terms of  $S_{21}$  bandwidth, as they do not vary too much in the UWB band, except the notch WLAN band. This characteristic can be considered satisfactory from  $S_{21}$  bandwidth point of view. Therefore the potential interference between UWB system and wireless systems working on WLAN band can be suppressed effectively. The normalized radiation patterns at 3 and 7.5 GHz are plotted in Figures 9(a) and (b). Figure 9(a) plots the  $E$  plane ( $XOZ$  plane) and the  $H$  plane ( $YOZ$  plane) pattern is given in Figure 9(b).

### 3.2. Parametric Study of Antenna-B

The effect of parametric variation on the frequency notch is investigated. The results of parametric variation are summarized in

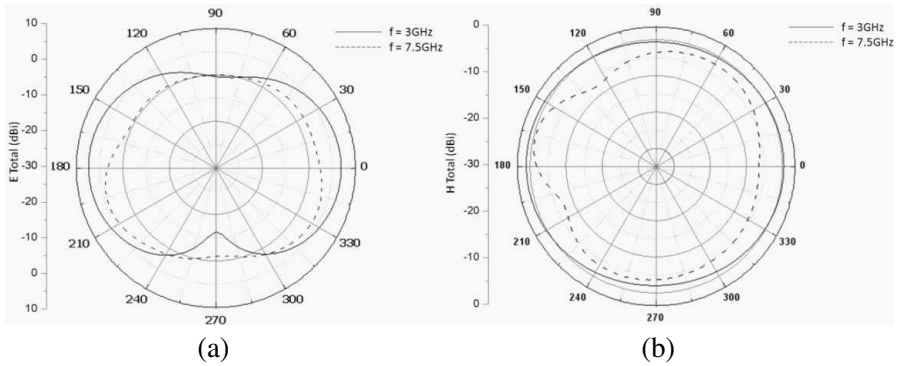


**Figure 9.** (a)  $E$  plane pattern and (b)  $H$  plane pattern for antenna-B.

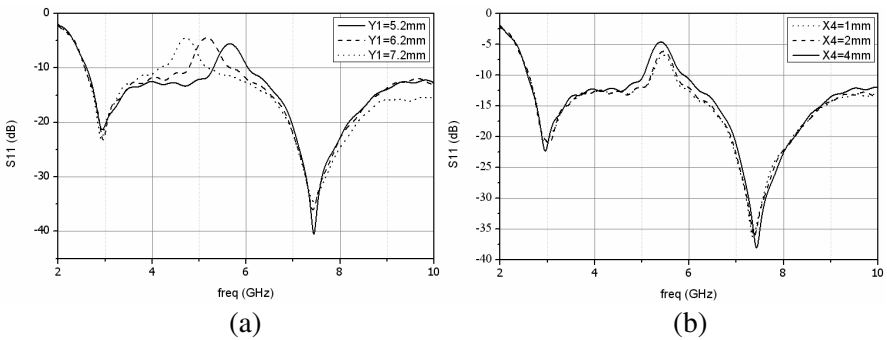


**Figure 10.** Parametric Variation: Return loss characteristics with U-slot parameter (a) with U-slot length and (b) U slot position on the patch.

Figures 10(a) and (b). From Figure 10(a), it is observed that the center frequency of the notch basically depends upon the total length of U-slot. The length of U-slot is almost half a wavelength at the notch center frequency. Thus notch center frequency shifts towards lower side on the frequency scale upon increasing the value of U-slot height. It is also noted that the total length of U-slot controls the notch center frequency, while the return loss characteristics in rest of the UWB band remains the same. It is also noted that, the notch bandwidth is not a function of total slot length. The notch characteristics also depends upon the U-slot offset ( $X_4$ ) from the patch center which is shown in Figure 10(b). For low values of “ $X_4$ ” the WLAN rejection is observed to be poor and also the notch bandwidth is less. While for its greater values the rejection is improved and the notch bandwidth is increased.

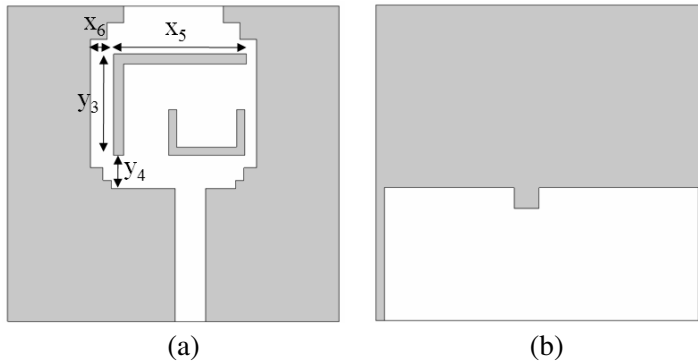


**Figure 11.** Geometry of proposed UWB antenna with dual notch (antenna-C). (a) Top view. (b) Bottom view.

**Table 3.** Parameters of L-shaped slot (all dimension in mm).

$X_5$	$X_6$	$Y_3$	$Y_4$
16	2.8	12.2	4

#### 4. UWB ANTENNA WITH DUAL FREQUENCY BAND NOTCH

The geometry of the third version of the UWB antenna (designated as antenna-C) is shown in Figure 11. An L shaped slot is additionally introduced to avoid the potential interference of 3.3 GHz–3.6 GHz frequency band. The notch behaves as a filter to stop the frequency band with center frequency 3.4 GHz. The optimized values of the parameters of antenna-C are given in Table 3.

##### 4.1. Frequency Domain Characteristics of Antenna-C

Apart from the IEEE 802.11a and HIPERLAN/2 WLAN frequency bands, WiMAX services from 3.3 GHz–3.6 GHz are also operated in UWB band. Thus an antenna, designed to possess a non radiating behavior at both of these frequency bands can eliminate the requirement of additional filters in the design of the UWB system.

To achieve the dual notch response, another L-slot is introduced in the radiating element with the total dimension of the order of half wavelength at 3.4 GHz. Figure 12 shows the VSWR characteristics of the antenna. The CST results are validated using EM software HFSS [22]. A good agreement is obtained between the results obtained from two different EM solver techniques. The two frequency notches

are distinctly visible from the VSWR characteristics of antenna-C. One of the rejected frequency bands is 3.3 GHz–3.6 GHz band and another one is 5.1–5.8 GHz. At these two bands, the VSWR of the radiator are greater than 4. While in the frequency bands other than the rejected bands, the VSWR is almost constant and well below 2. The radiation characteristics of this antenna are depicted in Figures 14(a) and (b). As can be observed, the characteristic are quite stable and looks similar with that of the antenna-B.

To compute the transmission through antenna-C, two antennas are arranged in transmit-receive system in face to face configuration with a separation of 50 mm. The characteristics shown in Figure 13,

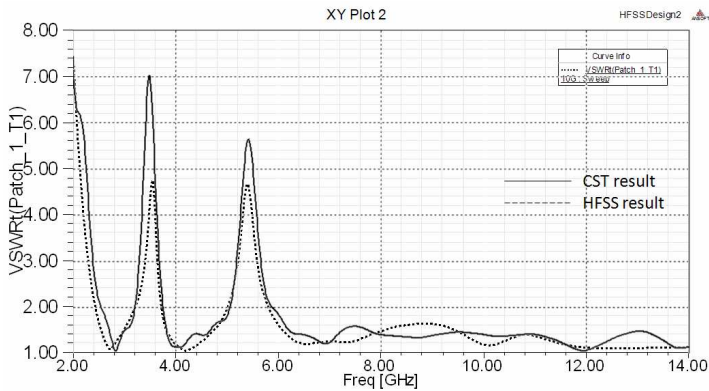


**Figure 12.** VSWR characteristics of antenna-C.

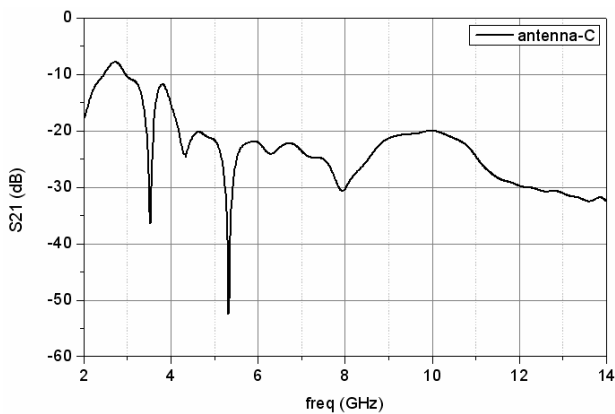


**Figure 13.** Insertion loss ( $S_{21}$ ) for antenna-C.

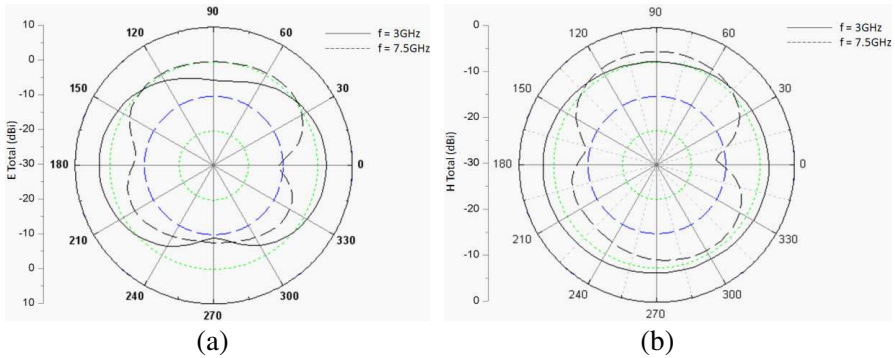


**Figure 14.** (a) *E* plane pattern and (b) *H* plane pattern for antenna-C.

clearly indicates two frequency bands for which the insertion loss is maximum and the reception is minimum.

### 5. TIME DOMAIN CHARACTERISTICS

The return loss characteristics and radiation patterns of the proposed UWB antennas (antenna-A, B and C) are given in last sections. Apart from the frequency domain characteristics which contain  $-10$  dB return loss and bandwidth, radiation pattern and gain, the time domain characteristics are also essential to characterize UWB antennas. The impulse responses of the proposed antennas are also studied. The arrangement of the calculation of the impulse response comprised of two identical antennas. The transmitter and receiver are positioned face to face, with a distance of 30 mm. A 5th derivative of the Gaussian pulse is a single pulse with the most effective spectrum under the FCC limitation floor, and this pulse can be transmitted without any fluttering [17]. Thus the same is used as source signal to drive the transmitter as given in Equation (2).

$$GM_5(t) = A \left( -\frac{t^5}{\sqrt{2\pi}\sigma^{11}} + \frac{10t^3}{\sqrt{2\pi}\sigma^9} - \frac{15t}{\sqrt{2\pi}\sigma^7} \right) \exp\left(-\frac{t^2}{2\sigma^2}\right) \quad (2)$$

where  $A$  is a constant chosen to meet the limitation set by FCC [17] and  $\sigma$  has to be 51 ps to satisfy the FCC limitation. The envelope of this pulse determines the shape of its spectrum.

From Figure 15(b), it is observed for antenna-B that the time delay between the transmitting antennas input pulse and the received antennas output pulse is about 0.75 ns. It is also observed that for antenna-B, the ringing is comparatively less than the antenna-A. As

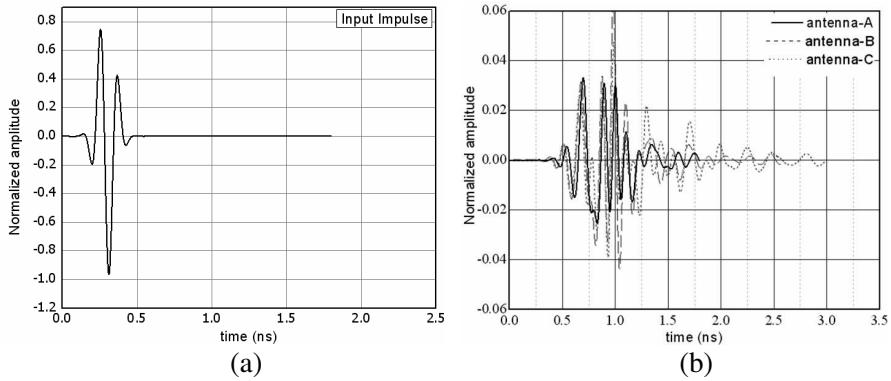


**Figure 15.** Time response characteristics comparison. (a) Transmitting antennas input. (b) Receiving antenna output for proposed antennas.

per the guideline recommended for UWB by FCC, the UWB system should work upto 500 Mbps, requiring the received pulse to be less than 2 ns in duration. The effective pulse width of the received impulse signal for the U-slot antenna is near about 1.2 ns that is ringing dies down before 1.2 ns, which is sufficient for data transmission at 500 Mbps. On the other hand, for antenna-C, the ringing duration is more than that of antenna-B. The effective pulse width for antenna-C is 2.25 ns, which means the antenna is usable upto 445 MHz without pulse distortion.

The time response of the antenna system may vary in different directions. To have a quantitative measure of the pulse distortion for face to face orientation between antenna pair, signal fidelity is used as a figure of merit [18–20]. Signal fidelity is the correlation coefficient between normalized input and output pulses. For ideal transmission without distortion, it should be 1. For the UWB antenna with notch pulses the correlation coefficient can be calculated using following equation.

$$F = \max_{\tau} \left\{ \int_{-\infty}^{+\infty} L[\hat{s}_1(t)] \cdot \hat{s}_2(t + \tau) dt \right\} \quad (3)$$

where  $L$  is a linear operator and,

$$\hat{s}_1(t) = \frac{s_1(t)}{\sqrt{\int s_1^2(t) dt}} \quad \text{and} \quad \hat{s}_2(t) = \frac{s_2(t)}{\sqrt{\int s_2^2(t) dt}}$$

$\tau$  is the delay for which is varied to make the numerator a maximum.

**Table 4.** Correlation factor for proposed UWB antennas.

Antenna-A	Antenna-B	Antenna-C
0.8562	0.8924	0.7903

The correlation factor between transmitter antenna input signal and receiving antenna output signal for all three antennas are computed and are given in Table 4 for face to face orientation.

## 6. CONCLUSION

In this paper a printed UWB monopole antenna and its advance version for WLAN frequency notch and WLAN, WiMAX dual frequency notch has been investigated. The rectangular cut present in the upper side of the truncated ground plane improves the impedance matching over the entire frequency band. The U-slot gives WLAN frequency notch, while the L-slot results in WiMAX frequency notch. The transmission coefficient and correlation factor are also computed for face to face orientation of the proposed antennas. The transmission, propagation and radiation characteristics show that the antenna is a potential candidate for the UWB system which requires WiMAX and WLAN rejection.

## REFERENCES

1. FCC Report and Order for Part 15 Acceptance of Ultra Wideband (UWB) Systems from 3.1–10.6 GHz, FCC, Washington, DC, 2002.
2. Wu, Q., R. H. Jin, J. P. Geng, and M. Ding, "Printed omnidirectional UWB monopole antenna with very compact size," *IEEE Trans. Antennas Propag.*, Vol. 56, 896–899, Mar. 2008.
3. Cho, Y. J., K. H. Kim, D. H. Choi, S. S. Lee, and S. O. Park, "A miniature UWB planar monopole antenna with 5-GHz band-rejection filter and the time-domain characteristics," *IEEE Trans. Antennas Propag.*, Vol. 54, 1453–1460, May 2006.
4. Ma, T. G. and S. J. Wu, "Ultrawideband band-notched folder strip monopole antenna," *IEEE Trans. Antennas Propag.*, Vol. 55, 2473–2479, Sep. 2007.
5. Fontana, R. J., "Recent system applications of short-pulse ultra wideband (UWB) technology," *IEEE Transactions on Microwave Theory and Techniques*, Vol. 52, No. 9, 2087–2104, 2004.

6. First Report and Order, "Revision of part of the commissions rule regarding ultra wide band transmission system FCC02-48," Federal Communications Commission, 2002.
7. Licul, S., J. A. N. Noronha, W. A. Davis, D. G. Sweeney, C. R. Anderson, and T. M. Bielawa, "A parametric study of time-domain characteristics of possible UWB antenna architectures," *Proc. Vehicular Technology Conf.*, Vol. 5, Oct. 6–9, 2003.
8. Yazdanifard, S., R. A. Sadeghzadeh, and M. Ojaroudi, "Ultra-wideband small square monopole antenna with variable frequency band-notch function," *Progress In Electromagnetics Research C*, Vol. 15, 133–144, 2010.
9. Ghaziand, A., M. N. Azarmanesh, and M. Ojaroudi, "Multi-resonance square monopole antenna for ultra-wideband applications," *Progress In Electromagnetics Research C*, Vol. 14, 103–113, 2010.
10. Jiang, J.-B., Z.-H. Yan, and C. Wang, "A novel compact UWB notch-filter antenna with a dual-Y-shaped slot," *Progress In Electromagnetics Research Letters*, Vol. 14, 165–170, 2010.
11. Zakerl, R., C. Ghobadi, and J. Nourinia, "A modified microstrip-FED two-step tapered monopole antenna for UWB and WLAN applications," *Progress In Electromagnetics Research*, Vol. 77, 137–148, 2007.
12. Kalteh, A. A., R. Fallahi, and M. G. Roozbahani, "Design of a band-notched microstrip circular slot antenna for UWB communication," *Progress In Electromagnetics Research C*, Vol. 12, 113–123, 2010.
13. Tu, S., Y.-C. Jiao, Y. Song, B. Yang, and X. Wang, "A novel monopole dual band-notched antenna with tapered slot for UWB applications," *Progress In Electromagnetics Research Letters*, Vol. 10, 49–57, 2009.
14. Wang, L., W. Wu, X.-W. Shi, F. Wei, and Q. Huang, "Design of a novel monopole UWB antenna with a notched ground," *Progress In Electromagnetics Research C*, Vol. 5, 13–20, 2008.
15. Lin, C.-C. and H.-R. Chuang, "A 3–12GHz UWB planar triangular monopole antenna with ridged ground-plane," *Progress In Electromagnetics Research*, Vol. 83, 307–321, 2008.
16. Kraus, J. D., R. J. Marhefka, and A. S. Khan, *Antenna and Wave Propagation*, 4th Edition, McGraw-Hill, 2006.
17. Yang, Y.-Y., Q.-X. Chu, and Z.-A. Zheng, "Time domain characteristics of band-notched ultrawideband antenna," *IEEE Trans. Antennas Propag.*, Vol. 57, No. 10, Oct. 2009.



18. Sheng, H., P. Orlik, A. M. Haimovich, L. J. Cimini, and J. Zhang, "On the spectral and power requirements for ultra-wideband transmission," *IEEE Int. Conf. on Communications*, Vol. 1, 738–742, Anchorage, AL, USA, Mar. 2003.
19. Lamensdorf, D. and L. Susman, "Baseband-pulse-antenna techniques," *IEEE Antennas Propag. Mag.*, Vol. 36, No. 1, 20–30, Feb. 1994.
20. Klemm, M. and G. Tröster, "Characterization of small planar antennas for UWB mobile terminals," *Wireless Commun. Mobile Comput.*, Vol. 5, 525–536, Aug. 2005.
21. Computer Simulation Technology, CST studio suite 2010, [www.cst.com](http://www.cst.com).
22. High Frequency Structure Simulator (HFSS) version 13.0.0, Ansoft Corporation.